

# Metamaterial CRLH Structure-based Balun for Common-Mode Current Indicator

Sungtek Kahng\*, Jinil Lee\*, Koon-Tae Kim\*\* and Hyeong-Seok Kim†

**Abstract** — We proposed a new PCB-type ‘common-mode current( $I_c$ ) and differential-mode current( $I_d$ ) detector’ working for fast detection of  $I_c$  and  $I_d$  from the differential-mode signaling, with miniaturization effect and possibility of cheaper fabrication. In order to realize this device, we suggest a branch-line-coupler balun having a composite right- and left-handed(CRLH) one-layer microstrip phase-shifting line as compact as roughly  $\lambda_g/14$ . The presented balun obviously is different from the conventional bent-&-folded delay lines or slits on the ground for coupling the lines on the top and bottom dielectrics. As we connect the suggested balun output ports of the differential-mode signal lines via the through-port named U and coupled-port named L,  $I_c$  and  $I_d$  will appear at port  $\Delta$  and port  $\Sigma$  of the present device, in order. The validity of the design scheme is verified by the circuit-and numerical electromagnetic analyses, and the dispersion curve proving the metamaterial characteristics of the geometry. Besides, the examples of the  $I_c$  and  $I_d$  indicator are observed as the even and odd modes in differential-mode signal feeding. Also, the proposed device is shown to be very compact, compared with the conventional structure.

**Keywords:** Metamaterial, Balun, Common-mode current detection, Composite right- and Left-handed, Phase shifter.

## 1. Introduction

Taking a look at the electric and electronic equipment in the past, it was harder to carry due to the larger physical volume and weight, but it has been circumvented through innovative fabrication and material technologies tagging along with advanced design methodologies. One technology is to change separate functional circuitries to the multilayers of printed circuit board (PCB). Therefore, PCBs re found in almost every electronic device these days. Typically, A PCB has a densely population of digital and analogue blocks that are interconnected with SMTs, signal lines, and so on. Pulses are generated and delivered from the driver of the digital block to a receiving component along the signal paths as traces or vias through slots, and may be interfered by undesirable electromagnetic interactions, causing the common-mode current, ground-bounce and SI problems [1].

To make an effort to mitigate unwanted coupling, crosstalk and radiated emission for higher level SI, one metal line above the conducting ground as a transmission line is prone to pick up a noise from the nearby discontinuity and will be substituted by a pair of balanced metal lines. It is called differential-mode signal feeding

which makes sure the reduction or removal of the common-mode current generated from the imbalance between the signal line and the ground [2-4]. P. E. Fornberg reported that the non-ideal return current will influence the differential-mode signaling [2]. A fast computation method was given by S. Kahng to observe the occurrence and portion of the common-mode current from differential-mode lines [3]. In order to suppress the common-mode current due to the differential signals crossing the slit ground, H.-H. Chuang employed two quarter-wavelength stubs parallel to the slit on the ground [4].

To tackle the common-mode current( $I_c$ ) and its radiated emission from the differential signaling practice, it is required to evaluate  $I_c$  and  $I_d$  from the balanced feeding lines of a device. To detect  $I_c$  on a cable, RF clamp-on electric current probes can be adopted, where the probe needs to be positioned around the cable [5]. Similar to this case, magnetic material core loops are used to tell  $I_c$  from  $I_d$  of a line, and  $I_c$  will be suppressed by the magnetic field polarity as well as the direction of turns [6]. The working principle of a balun is addressed in [7], but this has to entail ferrites not as a flat component as in [5, 6]. On the contrary, a flat and integrated balun is given to produce a high CMRR(common mode rejection ratio) level, while it is not aimed at distinguishing  $I_c$  from  $I_d$  [8].

We here propose a small, flat, light  $I_c$  and  $I_d$  indicator to overcome the aforementioned shortcomings. This is a 4-port balun as a microstrip line device equipped with a CRLH phase shifting segment. The previous baluns have apertures on the PEC ground in several layers, which

† Corresponding Author: School of Electrical and Electronics Eng., Chung-Ang Univ., Korea. (kimcaf2@cau.ac.kr)

\* Department of Information & Telecommunication Eng., University of Inchoen, Korea. ({s-kahng, victorlee}@inchoen.ac.kr)

\*\* School of Electrical and Electronics Eng., Chung-Ang Univ., Korea. (andorr@naver.com)

Received: May 16, 2013; Accepted: November 12, 2013

renders them heavier and more costly [9, 10]. Kumar bends 2 transmission lines, loads them with discrete capacitors and couples them as in [11] where the design steps are not expressed. Nevertheless, the suggested balun is completely printable not needing loading elements and has a small CRLH 90°-phase shifter at the upper output of a 90°-difference branch-line coupler. This metamaterial-based balun has the through port named U and coupled port named L that are cascaded to the 2 differential-mode lines, and Port  $\Delta$  as an output of the balun will produce  $I_d$  dominantly, and Port  $\Sigma$  as the other output port of the balun will produce  $I_c$  mainly. Hence, to shed a light on the design scheme, we bring the specifications first, and the process starts from the circuitual configuration and formulae for the CRLH phase shifting segment plugged into the balun's schematic comprising a branch-line coupler the phase shifter. This is confirmed by the circuit- and numerical electromagnetic analyses and the extraction of the dispersion diagram. To check the detection of the  $I_c$  and  $I_d$ , we excite the device at the even- and odd modes. Let alone, it is mentioned that the proposed design has effective size-reduction, compared to the conventional method.

## 2. Proposed Metamaterial Phase Shifter and Compact Balun

$I_c$  and  $I_d$  detection is performed by the balun that is connected to the differential-mode signal lines as given in Fig. 1. The 180°-phase difference between Through and Coupled ports is created by the balun with Port  $\Delta$  as the input, Port  $\Sigma$  terminated, and additional phase deviation by 90° from the upper output(Through) of the branch-line coupler. According to the conventional technique, the quarter-wavelength segment is attached to the output port for the further 90°-phase change which results in the growth in the size, inter-output imbalance, and insertion loss. To attack the drawback, we put the non-linear dispersive metamaterial characteristic to use as practiced in [12-14] that brings us effective size-reduction from adding a quarter-wavelength. For your notes, like [12-14], the compact phase shifter is a

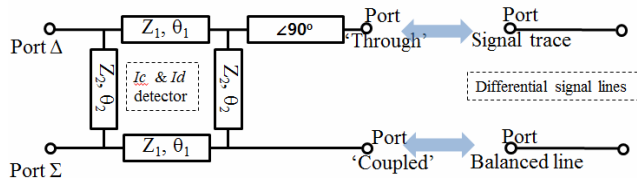


Fig. 1. Balun cascaded to the differential-mode signal lines.

Table 1. Specifications on the suggested balun design.

Items	Values
Band	1.2GHz ~ 1.7GHz
Return loss ( $ S_{11} $ )	$\leq -15$ dB
Outputs ( $ S_{21} ,  S_{31} $ )	$\leq -3\pm 1$ dB
Isolation ( $ S_{23} $ )	$\leq -15$ dB
Phase difference	180°

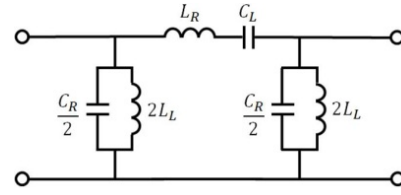


Fig. 2. Equivalent circuit of the CRLH phase shifter.

CRLH resonator that enables the device to meet the required phase change at the target frequency, and has the zeroth order resonance (ZOR) for remarkable. Prior to designing the metamaterial phase shifter-embedded balun, the specifications are introduced in the table below.

Particularly, we want the balun to be potentially used for an LTE band, for example, 1.2GHz~1.7GHz. As presented in Fig. 1, Port  $\Delta$  is the input port with Port  $\Sigma$  as the terminated port, and Port Through and Port Coupled are designated as output ports 2 and 3, where  $|S_{11}|$ ,  $|S_{21}|$ ,  $|S_{31}|$  and  $|S_{23}|$  should be  $\leq -15$ dB,  $-3$ dB,  $-3$ dB and  $\leq -15$ dB, respectively in the band. Most importantly,  $|\angle S_{31} - \angle S_{21}|$  should be 180° at 1.5GHz, as the balun. To meet the specifications above, the CRLH phase shifter is to generate the 90°-phase deviation and plugged into the branch-line coupler output. Reminding that the ZOR (no phase variation) of the CRLH geometry is instrumental to shortening the overall size, the 90°-phase change should occur at frequency(1.5GHz in this paper) and the ZOR at another frequency(2GHz in this paper). Ahead of the acquisition of the  $L$ 's and  $C$ 's, the building block circuit of the 90°-phase shifter is assumed like the following.

RH resonance is explained by  $L_R$  and  $C_R$ , while LH resonance goes with  $L_L$  and  $C_L$ , the details of which are elaborated on in [12-14]. Because of the LH property coexisting with the RH characteristics, the dispersion diagram has a non-linear curve that ZOR is created by the combination of the negative propagation constant with the positive one. If the proposed CRLH device makes +90° at port 2, while port 2 has 0° with -90° at port 3, ports 2 and 3 have the 180° phase difference in between. So, the  $L$ 's and  $C$ 's are formulated as the following, taking into account 90° at  $\omega_1(=2\pi f_1)$  and 0° at  $\omega_2(=2\pi f_2)$ .

$$L_R = \frac{Z_c [\beta_2 - \beta_1 \frac{\omega_1}{\omega_2}] (-Np)}{N\omega_2 [1 - (\frac{\omega_1}{\omega_2})^2]} \quad (1)$$

$$C_R = \frac{[\beta_2 - \beta_1 \frac{\omega_1}{\omega_2}] (-Np)}{N\omega_2 Z_c [1 - (\frac{\omega_1}{\omega_2})^2]} \quad (2)$$

$$L_L = \frac{NZ_c [(1 - (\frac{\omega_1}{\omega_2})^2)]}{\omega_1 [\beta_2 (\frac{\omega_1}{\omega_2}) - \beta_1] (-Np)} \quad (3)$$

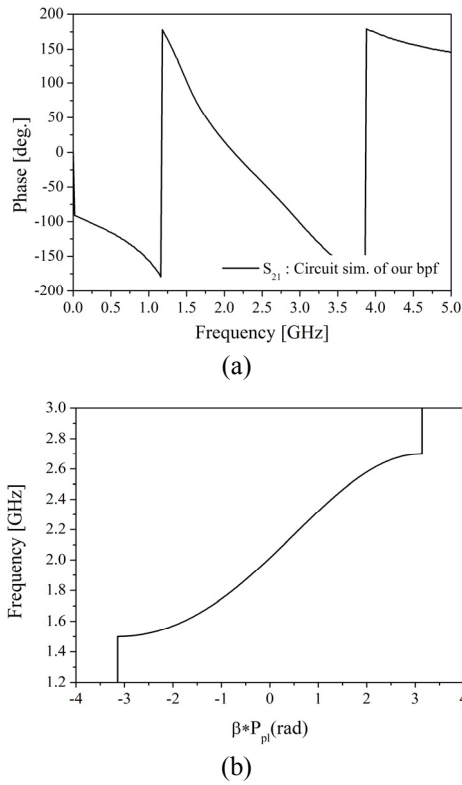


**Fig. 3.** Phase and dispersion of the CRLH phase shifting circuit; (a) phase: (b) dispersion diagram.

$$C_L = \frac{N[1 - (\frac{\omega_1}{\omega_2})^2]}{\omega_1 Z_c [\beta_2 (\frac{\omega_1}{\omega_2}) - \beta_1] (-Np)} \quad (4)$$

where  $\beta_i N p$  denotes the phase with  $N$  unit-cells, and we set  $N=1$  and the size of the unit cell  $p=\lambda_g/14$  for our design much less than one wavelength  $\lambda_g$ . By way of the equations above,  $C_R$ ,  $C_L$ ,  $L_R$  and  $L_L$  are obtained as 3.472 pF, 0.662pF, 8.681nH and 1.654nH, respectively. Based on the  $L$ 's and  $C$ 's, the phase vs. frequency relationship and the dispersion curve from S-parameters  $S_{21}$  and  $S_{11}$  are plotted.

The phase equals  $90^\circ$  at 1.5GHz as desired, and  $0^\circ$  occurs at 2GHz in Fig. 3(a). The  $180^\circ$ -phase difference between ports 2 and 3 will be examined at 1.5GHz, as this device is cascaded with the branch-line coupler. The metamaterial characteristics are seen as the non-linear dispersion curve covering  $\beta < 0$  (LH region) and  $\beta > 0$  (RH region) on the left and right sides of the ZOR at 2GHz. Now, the CRLH phase shifter above is substituted for the through port as Port 2.

The balun consists of the branch-line coupler and the compact metamaterial phase shifter as in Fig. 4(a).  $|S_{21}|$  and  $|S_{31}|$  are identical as -3dB, and  $|S_{11}|$  and  $|S_{41}|$  are less than -15dB at 1.5GHz, compliant with the specifications above as in Fig. 4(b). In terms of phase, the  $180^\circ$ -phase difference occurs between ports 2 and 3 as in Fig. 4(c). Hence, it is

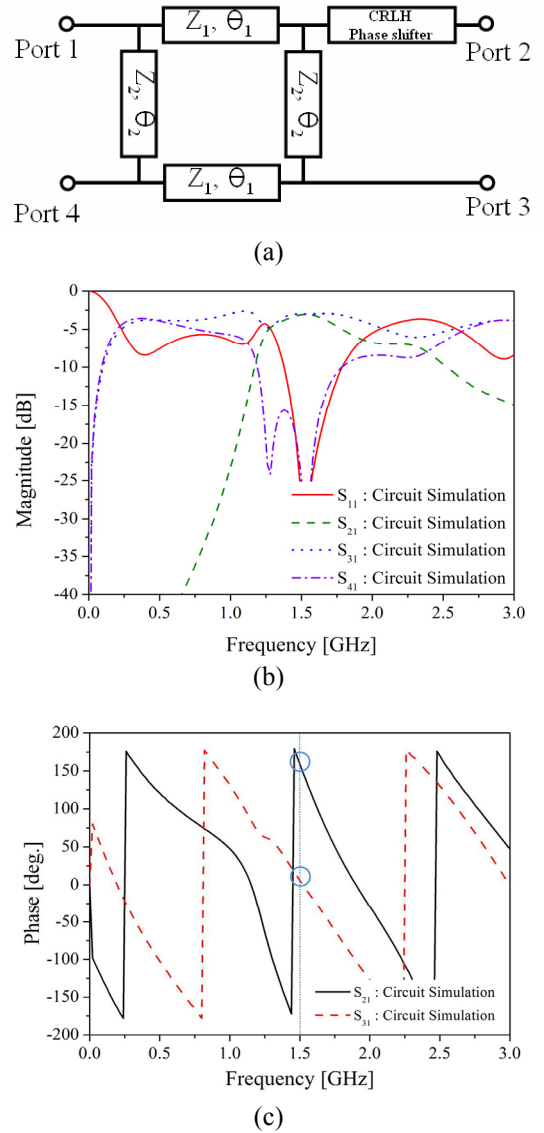


**Fig. 4.** Frequency response of the circuit simulation on our balun: (a) schematic; (b)  $|S_{11}|$ ,  $|S_{21}|$ ,  $|S_{31}|$  and  $|S_{41}|$  (c)  $\angle S_{21}$  and  $\angle S_{31}$ .

judged that the balun is designed correctly at this circuit level. Next, this equivalent circuit will be realized in the form of a physical structure.

Fig. 5(a) shows the geometrical shape of the proposed balun. The interdigital coupled lines flanked by shorted stubs are used to implement the CRLH phase shifter corresponding to the aforementioned circuit as is performed in [12-14]. 45mm, 2.4mm, 1.2mm, 0.4mm, 0.3mm, 58mm, 27.7mm, 30mm, and 6.5mm are found for  $W$ ,  $W_1$ ,  $W_2$ ,  $F_w$ ,  $F_{gap}$ ,  $L$ ,  $L_1$ ,  $L_2$ , and  $F_l$ , respectively as the geometrical parameters. Noting that the length of the CRLH phase shifter is 7.5mm equivalent to  $\lambda_g/14$  with respect to 1.5GHz, the proposed scheme brings effective miniaturization. Utilizing a commercial electromagnetic analysis tool SEMCAD X [15],  $S_{11}$ ,  $S_{21}$ ,  $S_{31}$  and  $S_{41}$  are obtained and it is revealed that they are in good agreement

with the circuit-simulation. According to Fig. 5(b),  $|S_{21}|$  and  $|S_{31}|$  equal -3.2dB slightly affected by the substrate loss(FR4), and  $|S_{11}|$  and  $|S_{41}|$  are  $\leq -15$ dB, meeting the specifications. Besides, ports 2 and 3 have the  $180^\circ$ -phase

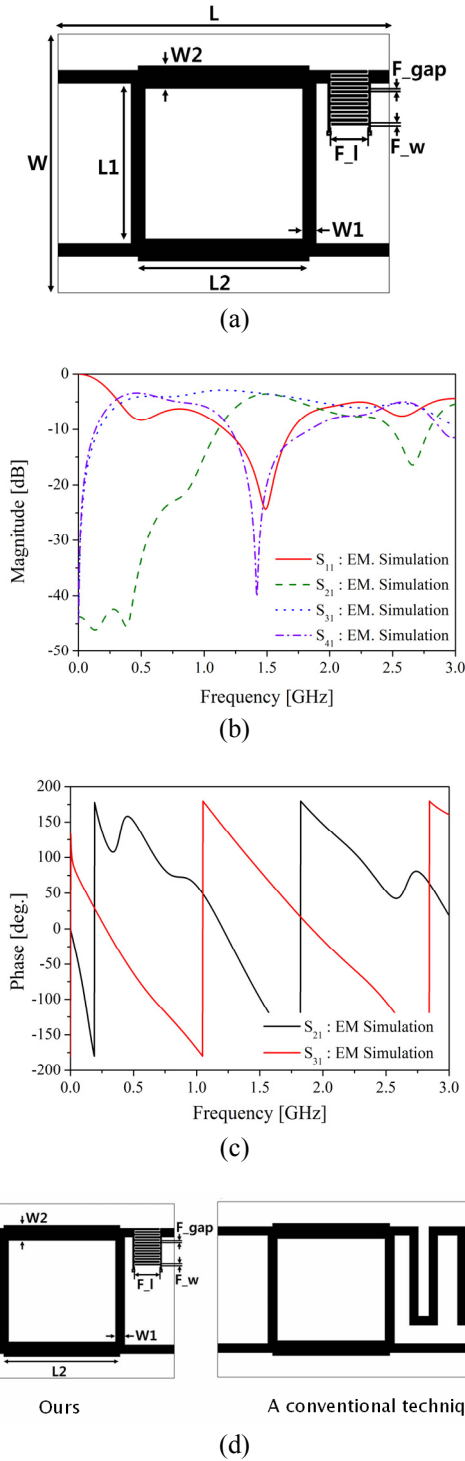


**Fig. 5.** Physical geometry of the suggested balun and its numerical electromagnetic simulation result as the frequency response: (a) physical structure; (b)  $|S_{11}|$ ,  $|S_{21}|$ ,  $|S_{31}|$  and  $|S_{41}|$ ; (c)  $\angle S_{21}$  and  $\angle S_{31}$ ; (d) size comparison.

deviation shown in Fig. 5(c). So, it is thought that the proposed device plays the role of the balun. Along with the electrical performance, as another feature of the proposed balun, its size reduction effect should be addressed. In Fig. 5(d), the present balun is smaller than the conventional one with the bent and folded segment. If the meandered part is made straight, it is apparent that the proposed CRLH-based geometry is the right choice for size-reduction compared to the other.

### 3. A 4-port Balun as A Common-mode Current Indicator

At present, applied to the common-mode current indicator, we assume the proposed balun plugged into the differential-mode signal lines as Fig. 1. Port 2, Port 3, Port 1 and Port 4 in Fig. 5(a) are mapped to Port U, Port L, Port  $\Delta$  and Port  $\Sigma$  of Fig. 1, in order. If differential-mode feed lines have  $I_d$  mixed with  $I_c$ , the top line (Port U) of the differential signal lines has  $I_c + I_d$ , and the other (Port L) has  $I_c - I_d$ . Then, Port  $\Delta$  receives  $2 \times I_d$  according to  $I_c + I_d - (I_c - I_d)$ , and Port  $\Sigma$  gets  $2 \times I_c$  by doing  $I_c + I_d + (I_c - I_d)$ . It implies that Port  $\Sigma$  indicates the common-mode current, and Port  $\Delta$  detects the differential-mode current about the injected input signals. To understand this scheme of the  $I_c$

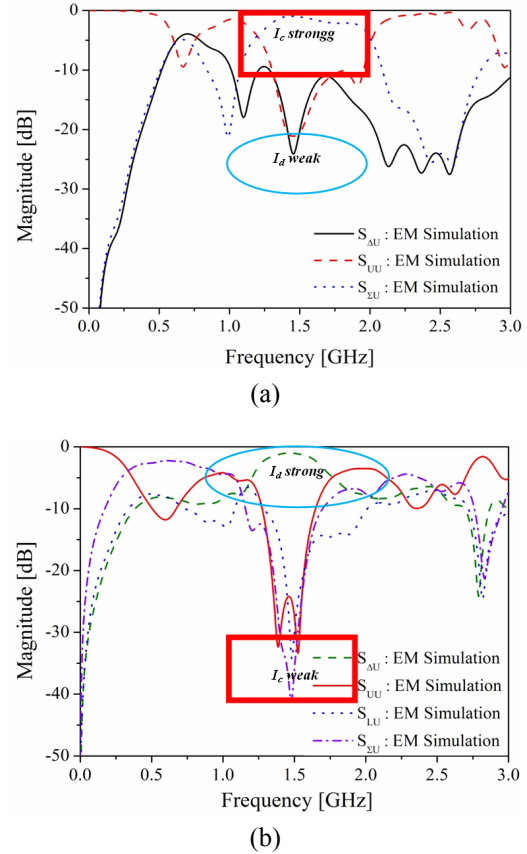


**Fig. 6.** Strength of  $I_c$  and  $I_d$  for the even- and odd-mode cases: (a) even-mode excitation; (b) odd mode.

and  $I_d$  indicator, two cases are taken that are the even- and odd modes in the differential signal lines. In the even-mode, Ports U and L both get  $I_c$ . Meanwhile, for the odd-mode,  $I_d$  enters Port, and  $-I_d$  is injected to Port L.

The even-mode implies the both of the differential signal lines have  $I_c$  equally. So,  $I_c$  at Port  $\Sigma$  makes strong, but  $I_d$  at Port  $\Delta$  becomes as weak as lower than -20dB. It is observed that the dotted curve as  $|S_{\Sigma U}|$  is the highest in Fig. 6(a), while the solid line as  $|S_{\Delta U}|$  in Fig. 6(a) is the lowest at 1.5GHz.

The ratio  $|S_{\Sigma U}|/|S_{\Delta U}|$  becomes very high and indicates the dominant factor of the inputs of the differential-mode signal lines is the common-mode current. Nonetheless, as to the odd-mode excitation, Port U gets  $I_d$ , and  $-I_d$  enters Port L, which leads to strong  $I_d$  at Port  $\Delta$ , and weak  $I_c$  at Port  $\Sigma$ . In other words, the dashed line as  $|S_{\Delta U}|$  in Fig. 6(b) is the highest, and the broken-line as  $|S_{\Sigma U}|$  in Fig. 6(b) is the lowest 1.5GHz. Then,  $I_c$  is ignorable, and strong  $I_d$  means the well-balanced condition for the differential signaling. Therefore, from the ratio  $|S_{\Sigma U}|/|S_{\Delta U}|$  of the proposed balun configuration, we are able to estimate the occurrence of the common-mode current in a differential-mode driven digital circuit and be ready to take steps for the common-mode current suppression.

#### 4. Conclusion

We have proposed a flat, light, and cheap common-mode current and differential-mode current indicator to do a prompt detection and estimation of  $I_c$  from  $I_d$  in differential-mode signal fed circuits. The advantages of our device are enabled by coping with a branch-line balun equipped with metamaterial one-substrate phase-shifter as compact as around  $\lambda_g/14$ . The suggested balun is applied to the differential-mode signal lines by way of Ports U and L,  $I_c$  and  $I_d$  appear at Ports  $\Delta$  and  $\Sigma$  of this structure, sequentially. The validity of the proposed scheme has been verified by the circuit- and electromagnetic numerical analyses, and the accompanying dispersion curve shows the metamaterial characteristics of the device. In addition, the examples of the  $I_c$  and  $I_d$  indicator have been observed as the even and odd modes in differential-mode signal feeding. Also, the proposed device is very compact, compared with the conventional structure.

#### Acknowledgements

This work was supported by the Incheon National University Research Grant. And the authors are indebted to Ms. Dajeong Eom with LG Electronics for her instrumental work and being considerate, and partly by Basic Science Research Program through the National Research Foundation of Korea (NRF) funded by the Ministry of

Education, Science and Technology (2012R1A1A2007758)

#### References

- [1] Howard Johnson, Martin Graham: High-Speed Signal Propagation – Advanced Black Magic. Prentice Hall, New Jersey, 2003.
- [2] P. E. Fornberg, M. Kanda, C. Lasek, M. Picket-May, and S. H. Hall, “The impact of a nonideal return path on differential signal integrity,” *IEEE Trans. on Electromagn. Compat.*, vol. 44, pp. 11-15, FEB. 2002.
- [3] S. Kahng, “Improved Differential Signaling of the DeCap-Loaded Rectangular Power-Bus With a Fast Calculation Method,” *IEEE Microwave and Wireless Components Letters*, vol. 16, no. 9, Sept 2006.
- [4] H.-H. Chuang, and T.-L. Wu, “A New Common-mode EMI Suppression Technique for GHz Differential Signals Crossing Slotted Reference Planes,” *Proceedings of 2010 IEEE International Symposium on Electromagnetic Compatibility*, pp. 12 - 15, 25-30 July 2010.
- [5] <http://www.hotconsultants.com/techtips/tips-cm.html>.
- [6] L. Nan, and Y. Yugang, “A Common Mode and Differential Mode Integrated EMI Filter,” *Proceedings of Power Electronics and Motion Control Conference*, pp. 1-5, 14-16 Aug. 2006.
- [7] <http://www.ham-radio.com/k6sti/balun.htm>.
- [8] C.-H. Chen, C.-H. Huang, T.-S. Horng, S.-M. Wu, J.-Y. Li, C.-C. Chen, C.-T. Chiu, and C.-P. Hung, “Integrated balun bandpass filter design with an optimal common mode rejection ratio,” *Proceedings of 2011 IEEE 61st Electronic Components and Technology Conference (ECTC)*, pp. 140-143, May-June 2011.
- [9] M. W. Katsube, Y. M. M. Antar, A. Ittipiboon, and M. Cuhaci, “A Novel Aperture Coupled Microstrip “Magic-T”,” *IEEE Microwave and Guided Wave Letters*, vol. 2, no. 6, pp. 245-218, June 1992.
- [10] M. Davidovitz, “A Compact Planar Magic-T Junction with Aperture-Coupled Difference Port,” *IEEE Microwave and Guided Wave Letters*, vol. 7, no. 8, pp. 217-218, August 1997.
- [11] B. P. Kumar, and G. R. Branner, “Optimized Design of Unique Miniaturized Planar Baluns for Wireless Applications,” *IEEE Microwave and Wireless Components Letters*, vol. 13, no. 29, Feb. 2003.
- [12] G. Jang, and S. Kahng, “Design of a dual-band metamaterial bandpass filter using zeroth order resonance,” *Progress in Electromagnetics Research C*, vol. 12, pp. 149-162, 2010.
- [13] G. Jang, and S. Kahng, “Design of a Metamaterial Bandpass Filter Using the ZOR of a Modified Circular Mushroom Structure,” *Microwave Journal*, vol. 54, no.5, pp. 158-167, 2011.
- [14] G. Jang, and S. Kahng, “Compact metamaterial zeroth-order resonator bandpass filter for a UHF band

and its stopband improvement by transmission zeros”  
*IET Microwave, Antennas Propagation*, vol. 5, no. 10,  
pp. 1175-1181, 2011.

[15] SEMCAD X by SPEAG, [www.speag.com](http://www.speag.com)



**Sungtek Kahng** He received his Ph.D. degree in electronics and communication engineering from Hanyang University, Korea in 2000, with a specialty in radio science and engineering. From 2000 to early 2004, he worked for the Electronics and Telecommunication Research Institute on numerical electromagnetic characterization and developed RF passive components for satellites. In March 2004, he joined the Department of Information and Telecommunication Engineering at the University of Incheon where he has continued research on analysis and advanced design methods of microwave components and antennas, including metamaterial technologies, MIMO communication, and wireless power transfer for M2M/cyber-physical systems



**Jinil Lee** He received his B.E. degree in 2012 and he is currently with the graduate school for his M.E. degree in the Incheon national university, Incheon, Korea. His research fields are microwave engineering, RF components, antennas, radars and metamaterials.



**Koon-Tae Kim** He received his B.S. degree in Information Telecommunication from Seo-Kyeong University and M.S. degree in electrical and electronics engineering from Chung-Ang University, South Korea in 2008 and 2010, respectively. He is working toward the Ph.D degree in electrical and electronics engineering at Chung-Ang University. His research interests are the design and optimization of passive components, and equivalent circuit modelling and analysis on RF components.



**Hyeong-Seok Kim** He received his B.S., M.S., and Ph.D. degrees from the Department of Electrical Engineering at Seoul National University, Seoul, Korea in 1985, 1987, and 1990, respectively. From 1990 to 2002, he was with the Division of Information Technology Engineering, Soonchunhyang University, Asan, Korea. In 1997, he was a Visiting Professor of the Electrical Computer Science Engineering, Rensselaer Polytechnic Institute, Troy, New York, USA. In 2002, he transferred to the School of Electrical and Electronics Engineering, Chung-Ang University, Seoul, Korea as Full Professor. His current research interests include numerical analysis of electromagnetic fields and waves, analysis, optimal design of passive and active components for wireless communication, RFID applications, power information technology, and electromagnetic education. He is a corresponding author in this paper.